

ACTIVE CONTROL OF SOUND TRANSMISSION THROUGH A DOUBLE PANEL PARTITION

P. SAS, C. BAO, F. AUGUSZTINOVICZ AND W. DESMET

*Department of Mechanical Engineering, Katholieke Universiteit Leuven,
Celestijnenlaan 300B, 3001 Leuven, Belgium*

(Received 4 February 1993, and in final form 29 November 1993)

The feasibility of improving the insertion loss of lightweight double panel partitions by using small loudspeakers as active noise control sources inside the air gap between both panels of the partition is investigated analytically, numerically and experimentally in this paper. A theoretical analysis of the mechanisms of the fluid–structure interaction of double panel structures is presented in order to gain insight into the physical phenomena underlying the behaviour of a coupled vibro-acoustic system controlled by active methods. The analysis, based on modal coupling theory, enables one to derive some qualitative predictions concerning the potentials and limitations of the proposed approach. The theoretical analysis is valid only for geometrically simple structures. For more complex geometries, numerical simulations are required. Therefore the potential use of active noise control inside double panel structures has been analyzed by using coupled finite element and boundary element methods. To verify the conclusions drawn from the theoretical analysis and the numerical calculation and, above all, to demonstrate the potential of the proposed approach, experiments have been conducted with a laboratory set-up. The performance of the proposed approach was evaluated in terms of relative insertion loss measurements. It is shown that a considerable improvement of the insertion loss has been achieved around the lightly damped resonances of the system for the frequency range investigated (60–220 Hz).

1. INTRODUCTION

Double panel partitions are often used in noise control engineering when relatively high insertion loss (*IL*) has to be achieved with lightweight structures: examples are mobile office partitions and aircraft fuselage shells. However, the performance of practical double panel structures rapidly deteriorates toward lower frequencies, at which it can even fall short of a single panel [1, 2]. The application of active noise control (ANC) methods can offer a viable solution in these cases.

The transmission of acoustic energy through any complex partition involves a number of fluid–structure interactions and coupling phenomena. In principle, any of these elements and/or conversion mechanisms can be influenced by means of active methods. For example, the sound radiation from an elastic plate into the free field can be controlled successfully by vibration actuators [3, 4]. Other studies have dealt with fluid–structure interactions in closed acoustic spaces (cavities). As a simple example, sound transmission through a flexible wall of a rectangular cavity was successfully controlled by a vibration control force [5]. Many research efforts have been mainly initiated by the challenge of noisy turboprop aircraft and submarine applications—some of them with considerable success—aimed at investigating the theory and application of active transmission control through cylindrical enclosures [6–11] by means of vibration control sources.

The aim of the approach proposed in this paper is to attempt to improve the insertion loss of an elementary double panel structure by means of small acoustical secondary sources, placed in the air gap between the panels. The basic idea of this approach is rather straightforward: the insertion loss of the investigated structure can be considerably improved if the sound field, assumed to be the main coupling element between the two panels of the structure, can successfully be attenuated by means of appropriately controlled secondary sources. Recently, such an approach has also been suggested elsewhere [12, 13].

In order to gain insight into the physical phenomena underlying the behaviour of a coupled vibro-acoustic system controlled by ANC methods, a detailed analysis of a fluid-structure interaction phenomena of the cavity and its boundaries is imperative. The detailed analysis, which is based on modal coupling theory [14, 15], has been reported in reference [16]. The most relevant conclusions are summarized in section 2, in particular those concerned with both the potentials and the limitations of an ANC system for the improvement of the *IL*.

The theoretical analysis is valid only for geometrically simple structures. For more complex geometries, numerical simulations are required. In section 3, a coupled FE-BE (finite element and boundary element) model is developed to predict the coupled vibro-acoustic behaviour of double panel structures. On the basis of this numerical model, the noise reductions which can be realized with the approach suggested are predicted.

To verify the conclusions drawn from the theoretical analysis and the numerical calculation and, more importantly, to demonstrate the potential of the proposed approach, experiments have been conducted with a laboratory set-up. Some of these results are presented in section 4.

2. THEORETICAL ANALYSIS

The aim of the theoretical analysis is to gain insight into the mechanism that governs the efficiency of the proposed approach, rather than to derive formulas in closed forms to calculate the *IL*. The analysis is restricted to the analytical description of the sound field in the air gap between the two panels. It is tacitly assumed that substantial attenuation of the sound pressure in the air gap will result in an increase of the *IL* of the whole system (the partition). This assumption is verified experimentally in the course of the measurements.

The active control of a sound field in a rigid walled enclosure with internal primary sources has been studied thoroughly by Nelson *et al.* [17-19]. The behaviour of the sound field in an enclosure bounded with flexible walls is expected to be considerably different, due to fluid-structure interaction.

The assumed configuration for the analytical model consists of two plane, parallel, flexible plates of the same (finite) size, clamped airtight to a rigid framework and baffled in an infinite rigid wall, as depicted in Figure 1. The analysis is based on the modal expansion method as given by Fahy [15], as the frequency range concerned lies well below the mass law region.

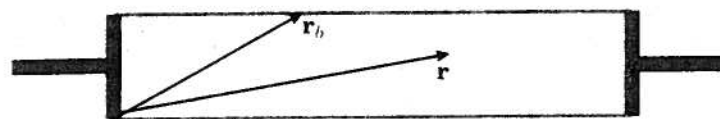


Figure 1. A sketch of the vibro-acoustic model.

The sound pressure p at any position \mathbf{r} in the cavity and at any time instant t is governed by the inhomogeneous wave equation

$$\nabla^2 p(\mathbf{r}, t) - (1/c^2) \partial^2 p(\mathbf{r}, t) / \partial t^2 = -\rho_0 (\partial q(\mathbf{r}, t) / \partial t), \quad (1)$$

where c is the sound speed in air, ρ_0 is the mean density of air and q represents the source volume velocity per unit volume (including the effect of the boundary surface vibration). As in the classical case of cavities with rigid boundaries [20], one can assume there, too, that the solution takes the form of an orthogonal modal expansion,

$$p(\mathbf{r}, t) = \sum_{n=0}^{\infty} \Phi_n(\mathbf{r}) P_n(t), \quad (2)$$

where Φ_n is the spatial characteristic function (i.e., the mode shape) of the n th mode of the cavity concerned, but with *rigid walls*, and P_n is the modal amplitude, representing the relative contribution of the n th *uncoupled* acoustic mode to the *coupled* solution. Φ_n is known *a priori*, while the P_n values are to be determined for the relevant system.

The vibrations of the plates (further referred to as the structure) are governed by the equation

$$D \nabla^4 w(\mathbf{r}_b, t) + m(\mathbf{r}_b) \partial^2 w(\mathbf{r}_b, t) / \partial t^2 = f(\mathbf{r}_b, t) + p(\mathbf{r}_b, t), \quad (3)$$

where D is the bending stiffness, \mathbf{r}_b represents any position on the plates, w is the displacement, m is the mass per unit area of the plate, f is the force input per unit area and p is the sound pressure on the plate (fluid loading). Again, the structural motion can be expressed as a weighted sum of modes of the uncoupled subsystem, Ψ_m , i.e., the *in vacuo* modes of the structure,

$$w(\mathbf{r}_b, t) = \sum_{m=1}^{\infty} \Psi_m(\mathbf{r}_b) W_m(t), \quad (4)$$

where W_m is the modal amplitude of the displacement.

For the sake of a more symmetrical formulation of the problem, the acoustic velocity potential v will be used instead of the sound pressure p , the relation between the two being

$$p(\mathbf{r}, t) = -\rho_0 (\partial v(\mathbf{r}, t) / \partial t). \quad (5)$$

Note that the velocity potential can also be expressed in a modal expansion form,

$$v(\mathbf{r}, t) = \sum_{n=0}^{\infty} \Phi_n(\mathbf{r}) \phi_n(t), \quad (6)$$

with $P_n(t) = -\rho_0 \dot{\phi}_n(t)$. Thus, the sound pressure can be expressed in terms of the modal expansion form of the velocity potential:

$$p(\mathbf{r}, t) = -\rho_0 \sum_{n=0}^{\infty} \Phi_n(\mathbf{r}) \dot{\phi}_n(t). \quad (7)$$

The solution for the unknowns ϕ_n and W_m can be determined from two infinite sets of algebraic equations (upon assuming harmonic time signals and neglecting damping), derived on the basis of equations (1)–(7):

$$A_{un}(\omega_{un}^2 - \omega^2) \phi_n - c^2 \sum_{m=1}^{\infty} j\omega C_{nm} W_m = -c^2 Q_n, \quad n = 0, 1, \dots, \infty, \quad (8)$$

$$A_{pm}(\omega_{pm}^2 - \omega^2)W_m + \rho_0 \sum_{n=1}^{\infty} j\omega C_{nm}\phi_n = F_m, \quad m = 1, \dots, \infty. \quad (9)$$

Here ω_{an} and ω_{pm} are the eigenfrequencies of the *uncoupled* acoustical and mechanical subsystems respectively, A_{an} is the generalized modal mass of the fluid, A_{pm} is the generalized modal mass of the structure, Q_n is the generalized source strength of the velocity sources inside the cavity, F_m is the generalized external mechanical force on the structure (if any), and C_{nm} is a dimensionless coupling factor, which is based on the geometrical similarity of the uncoupled modes of the structure and of the cavity on the common boundaries.

Now, if the number of the uncoupled acoustical modes considered is constrained to N and that of the structural modes to M , the algebraic equations (8) and (9) can be converted into a practical matrix form as

$$\begin{bmatrix} \Omega_a & \mathbf{A}_{ap} \\ \mathbf{B}_{pa} & \Omega_p \end{bmatrix} \begin{bmatrix} \phi \\ \mathbf{W} \end{bmatrix} = \begin{bmatrix} \mathbf{Q} \\ \mathbf{F} \end{bmatrix}, \quad (10)$$

where Ω_a and Ω_p are diagonal matrices with the eigenfrequencies of the *uncoupled* acoustical and mechanical subsystems, \mathbf{A}_{ap} and \mathbf{B}_{pa} are the coupling submatrices representing gyroscopic coupling, ϕ and \mathbf{W} are the modal amplitude vectors, and \mathbf{Q} and \mathbf{F} are the possible inputs of the system. The eigenfrequencies of the coupled system can be determined by setting \mathbf{Q} and \mathbf{F} to zero. The resulting matrix equation poses a non-standard eigenvalue problem, but this difficulty can easily be overcome by performing appropriate matrix transformations [21, 22]. Substituting the calculated eigenvalues back into the homogeneous version of equation (10) yields the freely vibrating coupled acoustic and structural modal amplitudes ϕ and \mathbf{W} for each eigenfrequency. The acoustic mode shapes of the coupled system, Φ_c , for example, can then be calculated as

$$\Phi_{ci}(\mathbf{r}) \approx \sum_{n=0}^N \Phi_n(\mathbf{r})\phi_{ni}, \quad i = 0, 1, \dots, N + M. \quad (11)$$

The physical interpretation of equations (10) and (11) is as follows.

From equation (10), due to a fluid–structure interaction and coupling (non-zero \mathbf{A}_{ap} and \mathbf{B}_{pa}), the resonance frequencies of the coupled system differ from those of the uncoupled system. Moreover, it has been found that the modal density of the coupled cavity is considerably higher than that of the uncoupled cavity. Thus, according to the study of Nelson *et al.* [17–19], more secondary sources are required to have a satisfactory global attenuation for the coupled system.

From equation (11), each mode shape of the *coupled* system comprises a number of mode shapes of the *uncoupled* system. It can be very similar to one of the uncoupled ones (even if their frequencies are highly different) or can be quite complex, depending on the modal amplitude weightings.

The effect of those coupling effects on the performance of ANC will be seen more clearly in section 4.3, where results of an experimental demonstration of the proposed approach with harmonic primary noise are presented.

3. NUMERICAL SIMULATION

3.1. THE NUMERICAL MODEL

The numerical model is based on a coupled FE–BE approach, with a dedicated software code [23]. In the calculation procedure the structure is modelled by finite elements, while the fluid is modelled by boundary elements, followed by an indirect variational

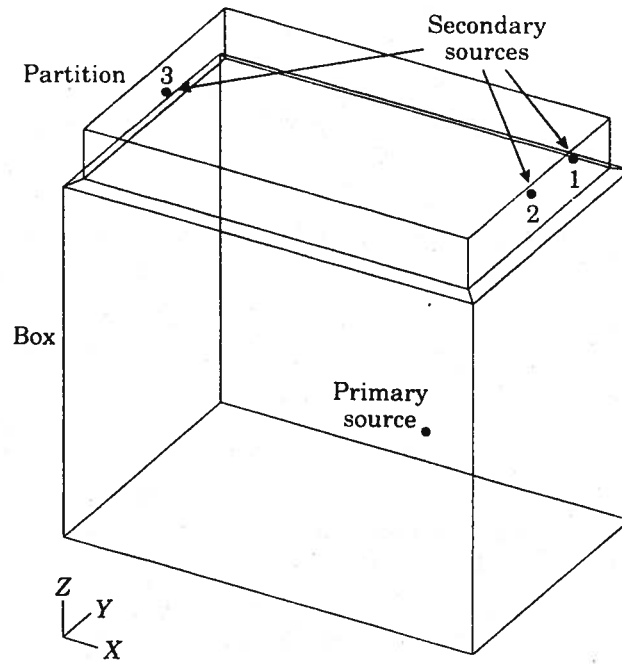


Figure 2. A sketch of the test set-up.

formulation. The displacements of the structure are projected to a previously calculated modal base of uncoupled structural mode shapes, resulting in a smaller system of equations. With this model, forced response calculations are performed for all frequencies of interest.

The model under study refers to a test set-up that will be described in detail in section 4. The set-up consists of two parts, a soundproof box and a double panel partition mounted on the top opening of the box (see Figure 2). The discretized test structure is shown in Figure 3. The mesh comprises 838 nodes and 870 linear quadrilateral and triangular shell elements. The double panel partition consists of two aluminium plates with

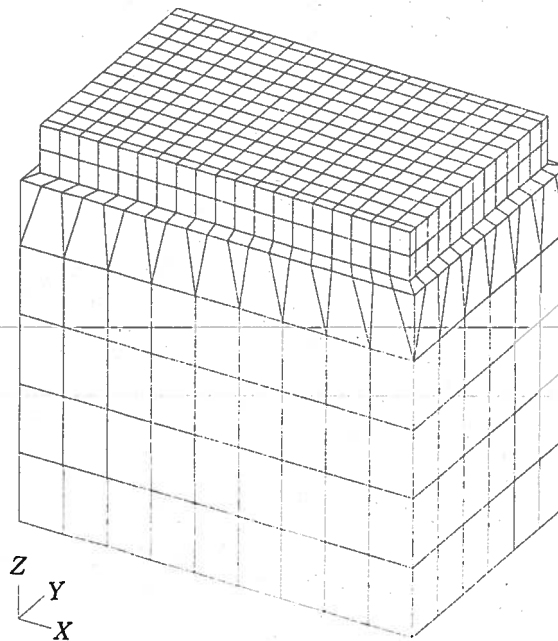


Figure 3. The mesh of the model in the numerical treatments.

dimensions of 1140×730 mm and a thickness of 1.5 mm, which are modelled with a density ρ of 2790 kg/m^3 , a Young's modulus of $70.6 \times 10^9 \text{ N/m}^2$ and a Poisson ratio ν of 0.33. The distance between the two plates is 150 mm. Both plates are considered to be clamped at their edges. The other boundaries of the test structure are assumed to be rigid and perfectly reflecting. The floor of the test structure is modelled as an infinite reflecting baffle. The structure is supposed to be excited by a (primary) acoustic point source inside the box, positioned somewhat off centre in the box. Two secondary acoustic point sources are placed inside the cavity of the partition. Three possible locations are considered, which are indicated in Figure 2. All sources are assumed to be velocity sources. The strength of the primary source is $1 \text{ m}^3/\text{s}$ and those of the secondary sources are dependent on ANC calculations.

3.2. CALCULATIONS OF POSSIBLE NOISE REDUCTIONS PROVIDED BY ANC

As stated in section 1, the basic idea of the proposed approach is to improve the *IL* of a double panel partition by means of controlling the sound field in the cavity between its two panels. Furthermore, it has been shown in section 2 that the control problem in the underlying situation is similar to that of a rigid wall enclosure containing internal sources only, which has been thoroughly studied by Nelson *et al.* [17–19]. Therefore the same control strategy to calculate the appropriate complex strengths of the secondary sources was adopted; i.e., minimizing the squared sound pressures at selected *control* points inside the cavity. After determination of the strengths of the secondary sources, a forced response calculation in the frequency range 55–220 Hz was performed with a frequency step of 0.5 Hz, for each source (both primary and secondary) separately. On the basis of the acoustic boundary layer results of the coupled FE–BE calculations, the sound pressure levels (*SPL*'s) for each frequency were calculated at 54 points located in a plane 150 mm above the upper plate. Finally, the *SPL*'s with ANC at those 54 points were obtained by superposition of the calculated primary and secondary sound pressure fields.

In Figure 4 is shown one of these calculated results, in which the two secondary sources were placed in locations 1 and 3 (see Figure 2) and the two control points inside the cavity of the partition. In Figure 4, the solid and the dashed line represent, respectively, the averaged *SPL* over the 54 points above the upper plate with and without ANC. Indeed, as anticipated, distinct noise reductions can be seen, especially at low frequencies and around the resonance peaks of the primary forced response.

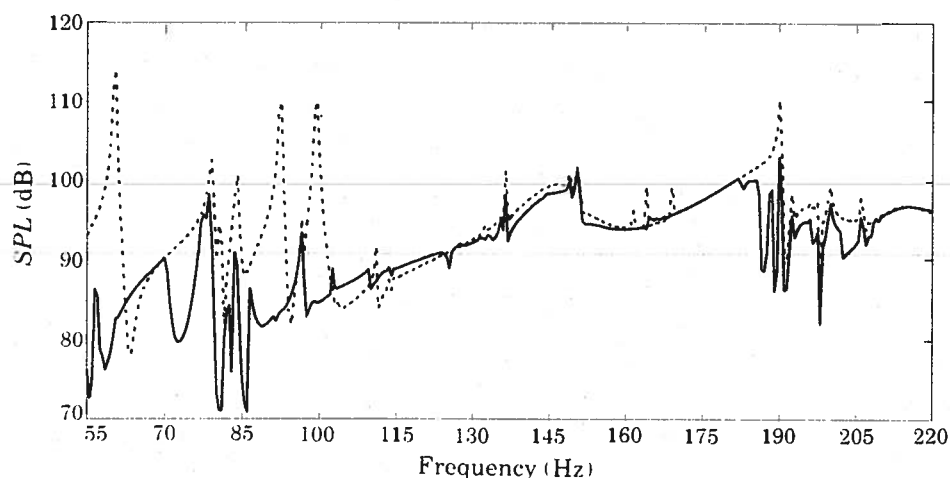


Figure 4. The calculated *SPL* averaged over 54 points at the radiating side of the partition with (—) and without (---) ANC.

4. ANC EXPERIMENTS ON THE DOUBLE PANEL

4.1. EXPERIMENTAL SET-UP

Mainly to demonstrate the potential of the proposed approach, experiments have been conducted with a laboratory set-up. The main structure of the set-up is a box with a double wall insulation, the cross-section of which is shown in Figure 5. The box was designed so that the insertion loss of the side walls of the box is at least 10 dB higher than that of the double panel partition to be tested (also taking into account the anticipated effect of the ANC system). The efficiency of the test box insulation was verified by performing a series of sound intensity measurements around the box by using a separate partition of extremely high insertion loss [24].

The double panel partition is formed by two plane, parallel aluminium plates of 1.5 mm thickness, clamped to a 10 mm thick and 150 mm high rectangular steel framework. The dimensions of the plates are 1140 × 730 mm. This partition is mounted in the open upper side of the box. To avoid air-borne and/or structure-borne flanking transmission, the partition is resiliently supported and carefully sealed. The partition is instrumented by an array of 42 microphones in the centre plane as well as 36 accelerometers on both plates. The microphone spacing is 120 × 127 mm in a 7 × 6 mesh, aimed at mapping the sound pressure distributions in the cavity within the frequency range of interest (below 220 Hz). The accelerometers are positioned in the central part of the plates, in a 6 × 6 mesh with 60 × 60 mm spacing to identify the vibration patterns. Two small sized, closed box commercial loudspeakers are fixed resiliently inside the cavity of the partition as the secondary sources. The incident noise is provided by means of a loudspeaker cube of six loudspeakers, placed inside the test box.

To compensate for possible variations of the characteristics in the system to be controlled, a multi-channel adaptive ANC controller has been used in the experiments [25]. In any type of adaptive algorithm, a performance index has to be optimized. Such an index should satisfy at least two essential requirements. First, the index should reflect the objective of the controller, which is to increase the insertion loss of the partition. Second, the index should be a function of the coefficients of the adaptive filters so that the index can be optimized by varying those coefficients. In our LMS (least mean squares) type

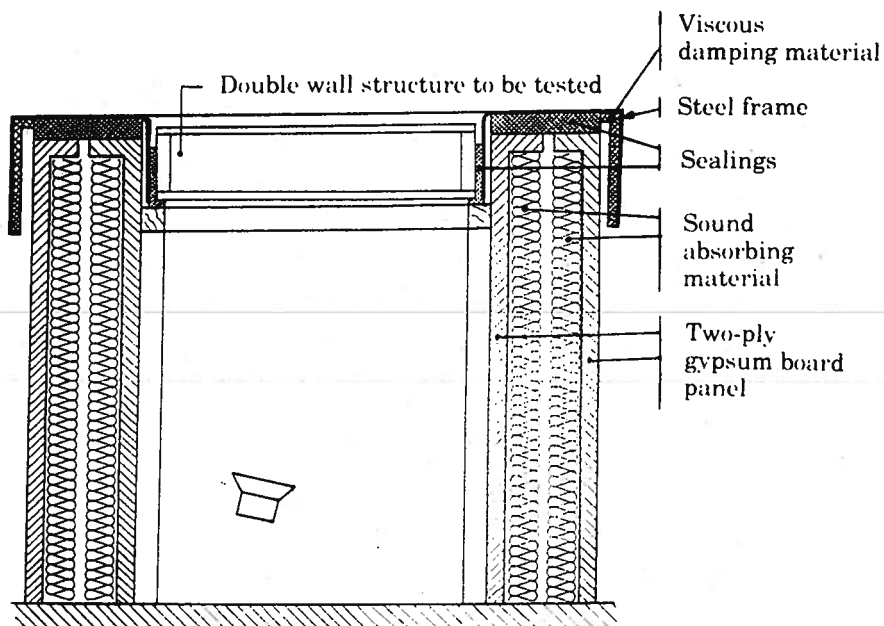


Figure 5. The cross-section of the test box in the experiments.

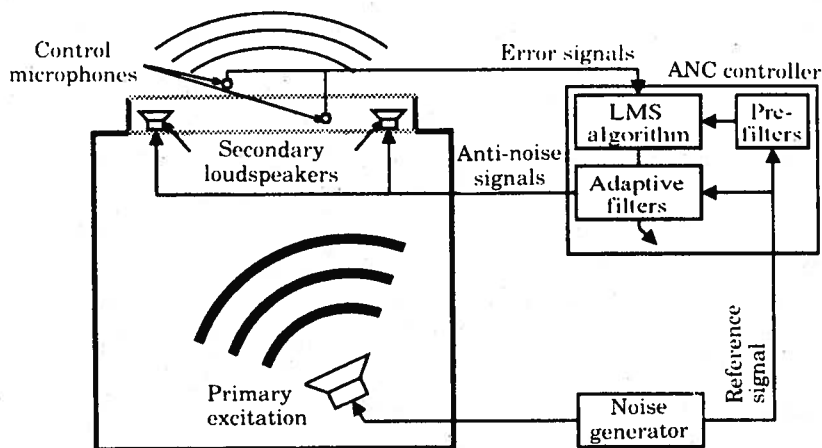


Figure 6. Schematic presentation of the laboratory set-up with the ANC system installed.

algorithm, the sum of the mean squared sound pressure time series, measured in control points by so-called error microphones, is chosen to be the index. As discussed in section 3.2, this index satisfies the first requirement. The index is also found to be a quadratic function of the coefficients of the adaptive filters. Thus, a straightforward gradient descent method is employed to derive iteratively the optimal set of the controller coefficients.

The ANC controller has been implemented on a PC based, commercially available digital signal processing board equipped with a TMS320C30 floating-point signal processor. The control algorithm was programmed in C-code. For most experiments a controller configuration with two loudspeakers and two microphones was used. The two secondary loudspeakers were fixed at opposite sides of the cavity. The error microphones (control points) could be relocated for different test conditions. The sampling frequency of the ANC system was set to 800 Hz, since the highest frequency of interest was 220 Hz. With such a sampling frequency, the adaptive algorithm in this implementation is capable of adapting 2×64 coefficients within one sampling interval, the number of coefficients in the fixed pre-filters being assumed to be 4×128 . The schematic presentation of the laboratory set-up with the ANC system installed is shown in Figure 6.

4.2. EXPERIMENTS WITH RANDOM PRIMARY NOISE

The experiments reported in this section refer to the condition in which the primary source was driven by a band-limited white noise signal (0–220 Hz). The performance of the proposed approach is evaluated on the basis of sound pressure measurements. Those measurements were performed in terms of *SPL* spectra at six selected field points 1 m from the partition (see Figure 7). The measured spectra were then averaged over those six points

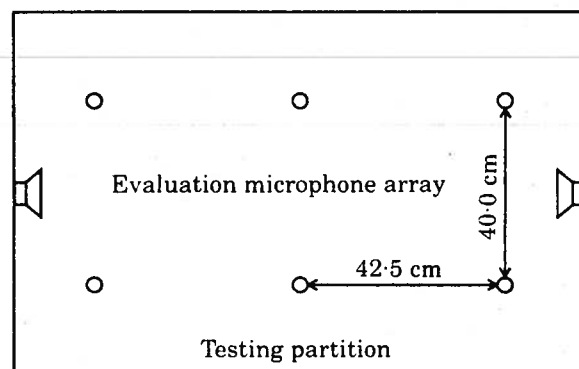


Figure 7. Positions of six evaluation microphones in the measurements (top view).

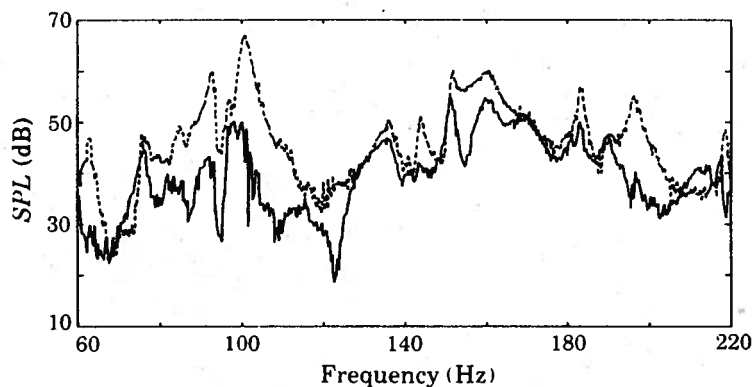


Figure 8. Measured *SPL* spectra averaged over six points 1 m from the partition, with random primary excitation. —, With ANC; ---, without ANC.

and compared with and without ANC. This yields a rough estimate of the improvement of the *IL* by the ANC system over any frequency band of interest.

In Figure 8 is shown the measurement result with two secondary loudspeakers and with control points inside the cavity of the partition (internal control points). Although the primary excitation is driven by a white noise signal, the transmitted sound field is dominated by the resonances of the cavity. With ANC, those resonance peaks in the *SPL* spectrum are considerably reduced. Between the resonances, the effect of ANC is less pronounced, but a noise reduction of 6.9 dB is still obtained over the frequency range 60–220 Hz. The result shows that the *IL* of the double panel partition is indeed improved by controlling the sound field inside the cavity of that partition.

It is of interest to explore the potentials of positioning the control points outside the partition (external control points) and to compare this with the previous result. The measurement results, with the control points 0.3 m and 0.9 m respectively above the partition, are given in Figure 9. The result with the internal control points is shown in the same figure to allow a comparison. It can be seen that the profiles of the *SPL* spectra of those three measurements are quite similar and the levels of the spectra are comparable except for a few frequency bands. Consequently, the overall noise reductions are also comparable, with a reduction of 7.7 dB for the control points 0.3 m above and 8.6 dB for the control points 0.9 m above, compared to 6.9 dB for the internal control points. Those results reveal that the improvement of the *IL* achieved by the proposed approach is largely due to the attenuation of the internal sound field of the partition, even in the case of external control points. Although the noise reductions with the external control points are

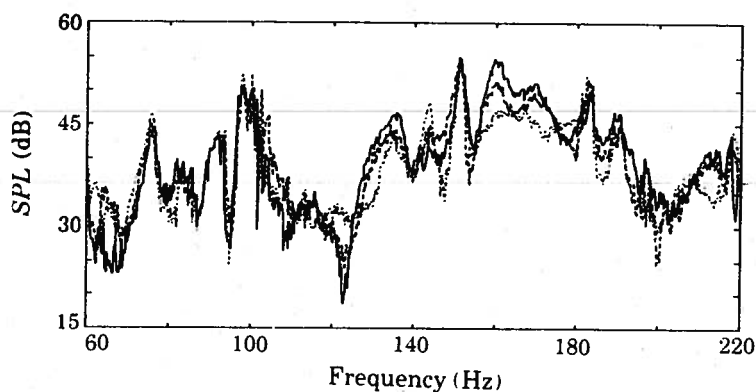


Figure 9. Measured *SPL* spectra averaged over six points 1 m from the partition, with different locations of control points. —, With internal control points; ---, with external control points 0.3 m above the partition; - · -, with external control points 0.9 m above the partition.

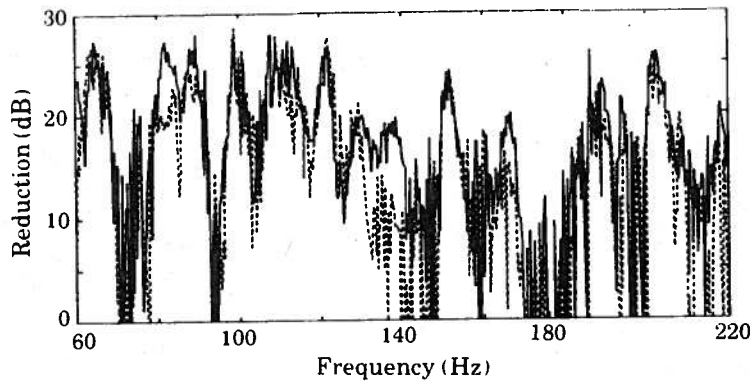


Figure 10. Spectra of noise reductions at a distance of 0.2 m (—) and at a distance of 1 m (---) from the partition (averaged over six points).

seen to be slightly higher, the internal configuration may sometimes be more attractive in practice for the following reasons. First, the internal configuration results in a more compact system. Second, in the internal configuration, the secondary transmission paths from the secondary loudspeakers to the control microphones, which play an important role in the controller design, are less sensitive to external changes.

To investigate the noise reduction in the area close to the partition, similar measurements were also conducted at a distance of 0.2 m from the partition. For those measurements, only the internal configuration was considered. The investigation has practical significance, as people have to stay close to partitions in some applications, such as in aircraft. The reductions at a distance of 0.2 m (solid line) and at a distance of 1 m (dashed line) are compared in Figure 10. It can be seen that the profiles of both reduction spectra are quite similar and the levels of reductions are comparable except for a few frequency bands in which the reduction at 0.2 m is higher. The overall noise reduction at 0.2 m is 8.4 dB, compared to 6.8 dB at 1 m.

4.3. EXPERIMENTS WITH HARMONIC PRIMARY NOISE

To illustrate the importance of the modal characteristics of the system to the performance of ANC, experiments were also conducted in the condition where the primary source was driven by a pure tonal signal (single frequency). Again, the performance of ANC was evaluated on the basis of sound pressure measurements.

As shown in section 4.2, the averaged reduction of *SPL* over the six measurement points at a distance of 0.2 m from the partition is representative for the noise reduction in the far field. In order to reduce the number of measurement points for field measurements,

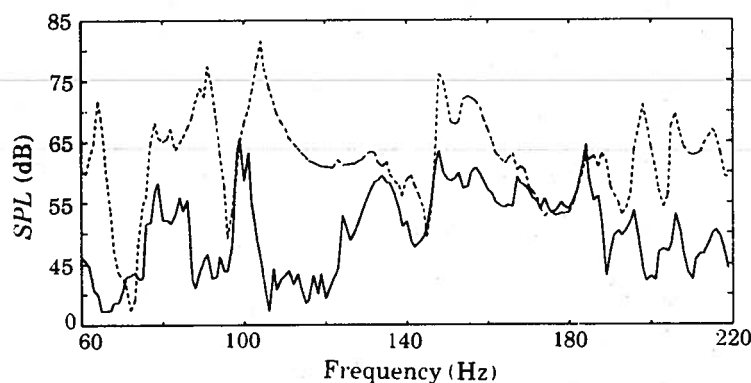


Figure 11. The measured *SPL* averaged over six points 0.2 m from the partition by using two secondary loudspeakers, against excitation frequencies. ---, Without ANC: —, with ANC.

all the measurements with the harmonic primary excitation were performed at a distance of 0.2 m from the partition. Also, the internal configuration was used.

In the first measurement series, the averaged *SPL* over six selected points (see Figure 7) was measured, with and without ANC. For these measurements, the primary excitation was chosen to be a stepped sinusoidal signal ranging from 60 Hz to 220 Hz with 1 Hz frequency steps and 20 second settlement period between the frequency increments.

The measurement result with two secondary loudspeakers is shown in Figure 11. As only a few modes are excited by the harmonic excitation, the internal sound field is much easier to attenuate (see section 2). Consequently, the noise reduction achieved with the harmonic primary excitation is considerably higher than that with the random primary excitation. It can be seen that substantial noise reductions are achieved around almost all resonance frequencies. At the highest resonance peak of 105 Hz, the noise reduction is more than 40 dB, resulting in a residual noise level comparable to the background noise level. Similar phenomena are observed around the resonance frequencies of 65 Hz and 92 Hz, where the noise reductions are higher than 30 dB. At other resonance frequencies, noise reductions of 10–20 dB can be seen. Noise reductions are lower (typically a few dB) at the anti-resonance frequencies and in the frequency bands between resonances. At some frequencies, a noise level increase of several dB can even be observed. However, this will not cause any serious problems in practice since the initial noise levels at those frequencies were already low. The slight increase of noise level at 185 Hz was due to inappropriate positioning of the control points. Indeed, a noticeable improvement has been achieved when other control points were used.

It is interesting to note that the result of the numerical simulation (Figure 4) is in agreement with the experimental result (Figure 10) for low frequencies (below 110 Hz). However, for higher frequencies the experimental result is considerably better than the simulation result. The primary reason for the difference is thought to be the fact that the damping ratio assumed in the numerical simulation is substantially smaller than that found in the experiment.

It is evident from Figure 11 that the noise reduction is strongly frequency dependent, even at resonance frequencies. This frequency dependence is more pronounced when only a single secondary loudspeaker is used, the result of which is shown in Figure 12. For instance, while almost 40 dB noise reduction is achieved at 92 Hz, a noise reduction of only a few dB is observed at 149 Hz, which is also a lightly damped resonance frequency.

This phenomenon is most likely caused by the complexity of the acoustic modes due to fluid–structure coupling, as pointed out by the theoretical analysis in section 2. To verify

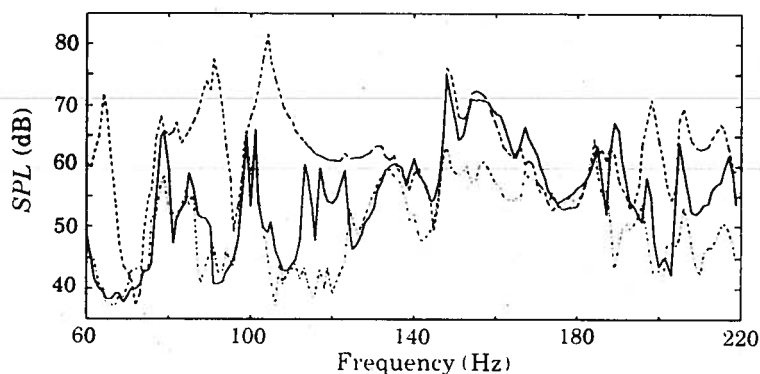


Figure 12. The measured *SPL* averaged over six points 0.2 m from the partition by using single secondary loudspeaker (comparing to the two loudspeaker case). ---, Without control; —, with single loudspeaker; -·-, with two loudspeakers.

TABLE 1
Acoustic modal characteristics of the partition obtained from the experimental modal analysis

Resonance frequency (Hz)	Damping ratio (%)	Mode shape	Resonance frequency (Hz)	Damping ratio (%)	Mode shape
65	0.62	[0,0,0]	156†	1.99	[1,0,0](1,1,0 + 3,1,0)
79†	1.52	[0,0,0 + (2,0,0)][(1,1,0 + 3,1,0)]	167†	0.67	[1,0,0] [(0,0,0 + 2,0,0)]
83†	0.46	[0,0,0 + (2,0,0)][(1,0,0)]	185	0.71	[0,0,0 + 2,0,0 + 0,2,0]
92	0.52	[0,0,0]	189†	0.33	[1,0,0] [(0,0,0 + 2,0,0)]
105	0.51	[0,0,0]	199	0.45	[1,0,0]
132†	1.08	[0,0,0 + (2,0,0)][(1,1,0 + 3,1,0)]	207†	0.41	[0,0,0 + (2,0,0)] [1,1,0 + 3,1,0]
142†	0.40	[0,0,0] [1,0,0 + (3,0,0)]	216†	0.47	[0,1,0 + 2,1,0] [1,0,0]
149†	0.80	[0,0,0 + 2,0,0] [1,0,0]			

† Pseudo-degenerate resonance.

this hypothesis, an extensive experimental modal analysis has been carried out for the test set-up. First, a modal model of the acoustic behaviour of the cavity was established based upon experimental frequency response function (FRF) data. Next, by resorting to those analytical calculations [26] that are based on the method presented in section 2, the modal characteristics at each resonance frequency were identified. Finally, the primary and the secondary forced responses were also calculated from the modal model.

The established modal characteristics of the cavity are summarized in Table 1. Unlike in the rigid wall case where only one single cavity resonance (the (1,0,0) mode at a frequency of 149 Hz) falls into the frequency range concerned, a number of cavity modes can be found due to fluid-structure coupling. These coupled modes are composed of a different number of uncoupled cavity modes as has been shown by the theoretical analysis in section 2. The identifiable constituent modes and their relative amplitudes are displayed in Table 1. For example, the notation $[0,0,0 + (2,0,0)]$ means that a particular mode is strongly affected by the (0,0,0) and to a lesser extent by the (2,0,0) uncoupled mode. Some of the experimentally found normal modes show the influence of another group of uncoupled modes. Such a kind of modal coupling is in principle impossible, as discussed, e.g. in references [19] and [26]. Nevertheless, the comparison of the experimental resonance frequencies with the theoretical calculations have revealed that in these cases two closely spaced separate resonances appear as one single resonance peak in the experimental FRF's. In Table 1, they are treated as if they were multiple roots in the eigenvalue problem, and are therefore referred to as the pseudo-degenerate resonance frequencies.

In order better to illustrate the information inherent in Table 1, some typical acoustic mode shapes are shown on the left side of Figure 13 for 105, 149 and 216 Hz, respectively. For comparison, in the right two columns of Figure 13 are shown the forced responses of the cavity for the same frequencies, calculated separately for the primary and for one secondary loudspeaker.

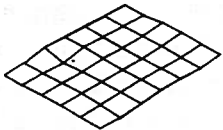
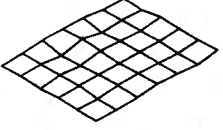
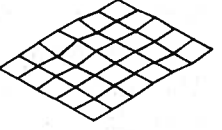
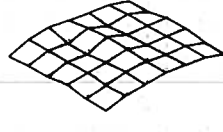
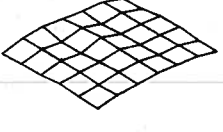
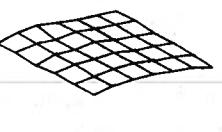
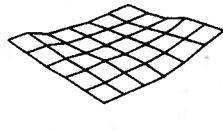
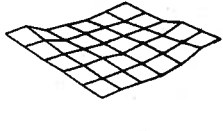
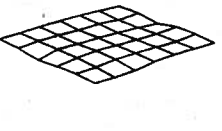
	Mode shape	Forced primary field	Forced secondary field
105 Hz	 (a)	 (b)	 (c)
149 Hz	 (d)	 (e)	 (f)
216 Hz	 (g)	 (h)	 (i)

Figure 13. A comparison of the acoustic mode shapes in the cavity of the partition, obtained from the experimental modal analysis, to the primary and the (single) secondary forced response fields at 105 Hz, 149 Hz and 216 Hz respectively.

even a small sound pressure increase can be seen in a certain region with the single loudspeaker configuration. The reason for this, as discussed above, is that due to the strong dissimilarity of the primary and secondary forced fields, the effect of the ANC system is apparently on the modification of the sound pressure pattern inside the cavity instead of on cancellation. Therefore noise reductions at the radiating side of the partition were not achieved.

5. CONCLUSIONS

The feasibility of improving the insertion loss of a lightweight double panel partition by using small loudspeakers as secondary sources inside the cavity between two panels has been investigated analytically, numerically and experimentally. It has been shown that a considerable improvement of the insertion loss of the double panel partition can be obtained by the proposed approach, provided that the sound field inside the cavity of the partition is substantially attenuated. For those situations in which the active control system has a pronounced influence on the modification of the sound pressure pattern inside the cavity rather than on the attenuation, the improvement of the insertion loss is not guaranteed.

The experiments in the laboratory have shown that the increase of insertion loss can be as high as 40 dB around the highest resonance peak of the system and about 30 dB for several other lightly damped resonances in the condition of harmonic primary noise. Positioning the control points outside the partition yields a slightly better result than explicitly controlling the sound field inside the cavity of the partition. However, the difference between the two results is not significant and the two results can be considered to be comparable for most frequencies.

ACKNOWLEDGMENTS

The work reported herein was partially performed in the framework of the EC Brite/Euram Research Project ASANCA (under contract AERO 0028-C). The project was supported by the Directorate-General for Science, Research and Development of the CEC.

REFERENCES

1. L. L. BERANEK and G. A. WORK 1949 *Journal of the Acoustical Society of America* **21**, 419–428. Sound transmission through multiple structures containing flexible blankets.
2. A. LONDON 1950 *Journal of the Acoustical Society of America* **22**, 270–279. Transmission of reverberant sound through double walls.
3. E. K. DIMITRIADIS and C. R. FULLER 1991 *American Institute of Aeronautics and Astronautics Journal* **29**(11), 1771–1777. Active control of sound transmission through elastic plates using piezoelectric actuators.
4. B. T. WANG, C. R. FULLER and E. K. DIMITRIADIS 1991 *American Institute of Aeronautics and Astronautics Journal* **29**(11), 1802–1809. Active control of structurally-radiated-noise using multiple piezoelectric actuators.
5. J. PAN, C. H. HANSEN and D. A. BIES 1990 *Journal of the Acoustical Society of America* **87**(5), 2098–2108. Active control of noise transmission through a panel into a cavity, I: analytical study.
6. H. C. LESTER and C. R. FULLER 1986 *AIAA Paper* 86–1957. Active control of propeller induced noise fields inside a flexible cylinder.
7. J. D. JONES and C. R. FULLER 1988 *Proceedings of 6th IMAC I*, 315–321. Reduction of interior sound fields in flexible cylinders by active vibration control.
8. S. D. SNYDER and C. H. HANSEN 1991 *Proceedings of Conference on Recent Advances in Active Control of Sound and Vibration*, 708–727. The effect of modal coupling characteristics on one mechanism of active noise control.

9. C. R. FULLER and J. D. JONES 1977 *Journal of Sound and Vibration* **112**, 389–395. Experiments on reduction of propeller induced interior noise by active control of cylinder vibration.
10. M. SALIKUDDIN and K. K. AHUJA 1989 *Journal of Sound and Vibration* **133**, 467–481. Application of localized active control to reduce propeller noise transmitted through fuselage surface.
11. D. R. THOMAS, P. A. NELSON, R. J. PINNINGTON and S. J. ELLIOT 1992 *Proceedings of the 14th AIAA Aeroacoustics Conference II*, 552–560. Active control of sound transmission through stiff lightweight composite fuselage constructions.
12. F. W. GROSVELD and K. P. SHEPHERD 1991 *29th AIAA Aerospace Science Meeting, AIAA-91-0498*. Active sound attenuation across a double wall structure.
13. L. GAGLIARDINI and P. BOUVET 1993 *Proceedings of Inter-noise 93 I*, 107–110. DAP: the active controlled double wall.
14. E. H. DOWELL, G. F. GORMAN III and D. A. SMITH 1977 *Journal of Sound and Vibration* **52**, 519–542. Acoustoelasticity: general theory, acoustic natural modes and forced response to sinusoidal excitation, including comparisons with experiment.
15. F. J. FAHY 1985 *Sound and Structural Vibration, Radiation, Transmission and Response*. London: Academic Press.
16. P. SAS, J. VAN DE PEER and F. AUGUSZTINOVICZ 1993 *Proceedings of the 14th AIAA Aeroacoustics Conference II*, 561–570. Modelling the vibro-acoustic behaviour of a double wall structure.
17. P. A. NELSON, A. R. D. CURTIS, S. J. ELLIOTT and A. J. BULLMORE 1987 *Journal of Sound and Vibration* **117**, 1–13. The active minimization of harmonic enclosed sound fields, part I: theory.
18. A. J. BULLMORE, P. A. NELSON, A. R. D. CURTIS and S. J. ELLIOTT 1987 *Journal of Sound and Vibration* **117**, 15–33. The active minimization of harmonic enclosed sound fields, part II: a computer simulation.
19. S. J. ELLIOTT, A. R. D. CURTIS, A. J. BULLMORE and P. A. NELSON 1987 *Journal of Sound and Vibration* **117**, 15–33. The active minimization of harmonic enclosed sound fields, part III: experimental verification.
20. P. M. MORSE and R. H. BOLT 1994 *Reviews of Modern Physics* **16**(2), 110–117. Sound waves in rooms.
21. J. PAN and D. A. BIES 1990 *Journal of the Acoustical Society of America* **87**(2), 691–707. The effect of fluid-structural coupling on sound waves in an enclosure—theoretical part.
22. L. MEIROVITCH 1974 *American Institute of Aeronautics and Astronautics Journal* **12**, 1337–1342. New method of solution of the eigenvalue problem for gyroscopic systems.
23. NUMERICAL INTEGRATION TECHNOLOGIES N.V. 1992 *SYSNOISE User's Manual, Revision 4.4*. Numerical Integration Technologies N.V., Belgium.
24. P. SAS, J. VAN DE PEER and F. AUGUSZTINOVICZ 1991 *Proceedings of 9th FASE Symposium on New Acoustical Measurement Methods*, 196–199. Development of an analysis procedure for the assessment of insertion loss characteristics of double wall structures.
25. C. BAO, P. SAS and H. VAN BRUSSEL 1992 *Journal of Sound and Vibration* **161**, 535–548. Adaptive active control of noise in 3-D reverberant enclosures.
26. P. SAS, F. AUGUSZTINOVICZ, W. DESMET and J. VAN DE PEER 1993 *Proceedings of ISAAC4*. Modelling the vibro-acoustic behaviour of a double wall structure.